Protective effect of 18β-glycyrrhetinic acid against H_2O_2-induced injury in Schwann cells based on network pharmacology and experimental validation

DI ZHANG[1*], JIANXIN SUN[1*], SHIQUAN CHANG[1], XING LI[1], HUIMEI SHI[1], BEI JING[1], YACHUN ZHENG[1], YI LIN[1], GUOQIANG QIAN[2], YUWEI PAN[3] and GUOPING ZHAO[1]

[1]College of Traditional Chinese Medicine, Jinan University, Guangzhou, Guangdong 510632; [2]College of Traditional Chinese Medicine, Guangdong Pharmaceutical University, Guangzhou, Guangdong 510006; [3]Preventive Treatment of Disease, Tianhe Traditional Chinese Medicine Hospital, Guangzhou, Guangdong 510665, P.R. China

Received May 28, 2021; Accepted August 3, 2021

DOI: 10.3892/etm.2021.10676

Abstract. The aim of the present study was to assess the protective effects of 18β-GA against hydrogen peroxide (H_2O_2)-induced injury. First, the SMILES annotation for 18β-GA was used to search PubChem and for reverse molecular docking in Swiss Target Prediction, the Similarity Ensemble Approach Search Server and the TargetNet database to obtain potential targets. Injury-related molecules were obtained from the GeneCards database and the predicted targets of 18β-GA for injury treatment were selected by Wayne diagram analysis. Subsequently, Kyoto Encyclopedia of Genes and Genomes analysis was performed by WebGestalt. The experimental cells were assorted into control, model, 10 μM SB203580-treated, 5 μM 18β-GA-treated and 10 μM 18β-GA-treated groups. Hoechst 33258 staining was performed and intracellular reactive oxygen species (ROS) levels, cell apoptosis, Bcl-xl, Bcl-2, Bad, Bax, cleaved-caspase 3, cleaved-caspase 7, transient receptor potential ankyrin 1 (TRPA1) and transient receptor potential vanilloid 1 (TRPV1) levels, as well as p38 MAPK phosphorylation were measured. The 'Inflammatory mediator regulation of TRP channels' pathway was selected for experimental verification. The results indicated that 10 μM 18β-GA significantly increased cell viability as compared with the H_2O_2-treated model group. As suggested by the difference in intracellular ROS fluorescence intensity, 18β-GA inhibited H_2O_2-induced ROS production in Schwann cells. Hoechst 33258 staining indicated that 18β-GA reversed chromatin condensation and the increase in apoptotic nuclei following H_2O_2 treatment. Furthermore, flow cytometry suggested that 18β-GA substantially inhibited H_2O_2-induced apoptosis. Pre-treatment with 18β-GA obviously reduced Bad, Bax, cleaved-caspase3, cleaved-caspase 7, TRPA1 and TRPV1 levels and p38 MAPK phosphorylation after H_2O_2 treatment and increased Bcl-2 and Bcl-xl levels. In conclusion, 18β-GA inhibited Schwann cell injury and apoptosis induced by H_2O_2 and may be a potential drug to prevent peripheral nerve injury.

Correspondence to: Professor Guoping Zhao, College of Traditional Chinese Medicine, Jinan University, 601 Huangpu Avenue West, Guangzhou, Guangdong 510632, P.R. China
E-mail: tguo428@jnu.edu.cn

Dr Yuwei Pan, Preventive Treatment of Disease, Tianhe Traditional Chinese Medicine Hospital, 9 Tangshi Road, Guangzhou, Guangdong 510665, P.R. China
E-mail: pywyvette@foxmail.com

*Contributed equally

Abbreviations: H_2O_2, hydrogen peroxide; ROS, reactive oxygen species; 18β-GA, 18β-glycyrrhetinic acid; TRPA1, transient receptor potential ankyrin 1; TRPV1, transient receptor potential vanilloid 1

Key words: 18β-glycyrrhetinic acid, hydrogen peroxide, H_2O_2, p38 MAPK, Schwann cells, network pharmacology

Introduction

18β-Glycyrrhetinic acid (18β-GA) and 18α-GA are the active components of *Glycyrrhiza glabra* (1). As the natural availability of the 18α-GA isomer is low and that of 18β-GA is higher, there is a greater research focus on 18β-GA (2). Previous studies have demonstrated the diverse favourable effects of 18β-GA, including its hepatoprotective, renoprotective, antioxidant and inflammation relief effects (3-5). Zhou *et al* (6) indicated that 18β-GA suppressed autoimmune encephalomyelitis by inhibiting the activation of microglia and facilitating remyelination via inhibition of the MAPK signalling pathway. Oztanir *et al* (7) suggested that treatment with 18β-GA for 10 days after cerebral ischaemia/reperfusion (I/R) altered the neurodegenerative effect of I/R on brain tissue due to its powerful antioxidant effect and capability to scavenge radicals. Kao *et al* (8) indicated that 18β-GA protected PC12 cells from 6-hydroxydopamine-induced harm through PI3K/Akt signalling and the Bcl-2 family. However, the protective mechanism of 18β-GA in Schwann cells has remained elusive. As Schwann cells have a vital impact on nerve repair (9), the present study explored the protective capacity of 18β-GA against H_2O_2-induced injury in Schwann cells.

Peripheral nerve injury is a common problem and may result in severe disability and an economic burden (10). Despite the fact that peripheral nerve cells have a specific regenerative ability, functional prognosis is not optimal (11). Schwann cells are proliferative glial cells in the peripheral nervous system and they are essential for nerve repair after injuries to maintain normal nerve function (12). Increasing evidence indicates that Schwann cell death is the major cellular event in the pathogenesis of peripheral nerve injuries, which tend to manifest in the form of apoptosis (13). In addition, oxidative stress after injury has a considerable role in neuronal death. The most important genes associated with apoptosis are proteins of the Bcl family and caspases (14,15). Su *et al* (3) indicated that 18β-GA lessened the severity of radiation-induced skin injury and decreased inflammatory infiltration and the levels of TNF-α, IL-1β and IL-6 in dermal tissues by decreasing NADPH oxidase activity and reactive oxygen species (ROS) production and suppressing the activation of p38 MAPK and NF-κB signalling. 18β-GA demonstrated considerable functions similar to those of Pyr3 or 2-aminoethyl diphenylborinate inhibitors and suppressed high glucose-induced effects, including the blockade of transient receptor potential (TRP) cation channel subfamily C member 3 (TRPC3) and TRPC6 protein expression and decreases in ROS and inducible nitric oxide synthase expression (16). Based on the determinant role of 18β-GA in inhibiting ROS generation and inflammatory infiltration, it was hypothesized that 18β-GA protects against nerve injury caused by hydrogen peroxide (H_2O_2). However, the mechanism of the neuroprotective effect of 18β-GA has so far remained elusive.

Network pharmacology has illustrated the synergistic effects and underlying mechanisms of herbs via network analysis, which is an appropriate way to measure the effectiveness and demonstrate the functional mechanisms of novel bioactive compounds. In the present study, network pharmacology was applied to identify related targets of 18β-GA for the treatment of neuronal injury and these targets were then experimentally verified. This experimental verification suggested that 18β-GA protected Schwann cells from H_2O_2-induced injury by inhibiting the phosphorylation of p38 MAPK.

Methods

Pathway prediction based on network pharmacology. The SMILES annotation for the drug 18β-GA was found in PubChem. After searching Swiss Target Prediction, the Similarity Ensemble Approach (SEA) Search Server and TargetNet (http://www.swisstargetprediction.ch, http://sea.bkslab.org and http://targetnet.scbdd.com/home/index, respectively), SMILES for monomer drugs was selected and the species was limited to *Homo sapiens*. The obtained protein targets and corresponding UniProt IDs were imported into Excel. By entering the keywords 'injury', 'damage' and 'harm' into the 'GeneCards database' (https://www.genecards.org), reported injury-related genes were acquired. The common targets of injury and 18β-GA were screened by Wayne diagram analysis. These targets were imported into the WebGestalt database (http://www.webgestalt.org/) and Kyoto Encyclopedia of Genes and Genomes (KEGG; https://www.genome.jp/dbget-bin/www_bget?pathway:map04750) pathway analysis was performed with $P<0.05$ and gene count ≥5.

Reagents and cell line. 18β-GA (cat. no. G109796; 98.0%) was acquired from Shanghai Aladdin Biochemical Technology Co., Ltd. PBS, Triton X, TBS and neutral balsam were purchased from Shuyan Biological Technology Co., Ltd. Trypsin was acquired from Guangzhou Saiguo Biological Co., Ltd. PageRμLer Prestained Protein Ladder and Marker (cat. no. P12083) were obtained from Shanghai Bioscience Technology Co. Ltd. SB203580 (a p38 MAPK inhibitor) was purchased from Selleck Chemicals. Polyvinylidene difluoride (PVDF) membranes were obtained from MilliporeSigma. Hoechst 33258 stain (cat. no. RYS580), phosphatase inhibitor cocktail 1 (cat. no. RBG2012) and a BCA protein content kit (cat. no. P0010S) were acquired from Guangzhou Junji Biotechnology Co., Ltd. RIPA buffer (cat. no. WB-0071) was purchased from Beijing Dingguo Biological Co., Ltd. Rabbit antibodies against TRP vanilloid 1 (TRPV1), TRP ankyrin 1 (TRPA1), β-actin, cleaved-caspase-3, cleaved-caspase-7, Bcl-xL, p38 MAPK, phosphorylated (p)-p38 MAPK, Bcl-2, Bax and Bad (cat. nos. ab6166, NB110-40763, 9662S, 9664S, 8438S, 2764S, 8690S, 4511S, ab117115, 2772 and 9292, respectively) were acquired from Guangzhou Juyan Biological Co., Ltd. Goat anti-rabbit secondary antibody (cat. no. CW0103) was acquired from Guangzhou Juyan Biological Co., Ltd. Meilunbio® ECL reagent (cat. no. MA0186-100ML) was acquired by Guangzhou Jiayan Biological Co., Ltd. A Cell Counting Kit-8 (CCK-8; cat. no. 96992) was acquired from Sigma-Aldrich (Merck KGaA). The Annexin V FITC Apoptosis Detection Kit I (cat. no. 556547) was obtained from Guangzhou Juyan Biological Co., Ltd. Diluted primary antibody, diluted secondary antibody, western blot transfer solution and western blot electrophoresis solution were obtained from Servicebio. RNAiso Plus was acquired from Takara Biotechnology, Co., Ltd. SYBR®-Green Premix qPCR, an Evo M-MLV RT-PCR kit and RNase-free water (cat. nos. AG11701, AG11602 and AG11012) were obtained from Accurate Biotechnology Co., Ltd. The Schwann cell line RSC96 was acquired from Shanghai Institute of Cell (cat. no. GNR6). The cell line used in the experiments was between passages 8 and 13.

Cell viability and cytotoxicity assays. The viability of Schwann cells was determined by the CCK-8 assay. First, Schwann cells were seeded into 96-well plates at a density of $6x10^3$ cells/well for 24 h. To assess H_2O_2-induced injury, cells were incubated with H_2O_2 at various concentrations (0, 20, 50, 100, 150, 200, 250 and 300 μM) for 4 h and then subjected to the CCK-8 assay. For the 18β-GA-mediated protection assay, Schwann cells were pre-treated with 18β-GA (0, 2.5, 5, 7.5, 10, 15, 20 and 30 μM) 24 h prior to being exposed to H_2O_2 (200 μM) for 4 h. After the incubation, the medium was discarded and the cells were then incubated with CCK-8 solution at 37˚C for 1 h. The absorbance (450 nm) was them measured by using a microplate reader (Bio-Tek Instruments, Inc.).

Experimental grouping. The experimental groups were as follows: Control, model (200 μM H_2O_2), 10 μM SB203580 (200 μM H_2O_2 + 10 μM SB203580), 5 μM GA (H_2O_2 200 μM + 5 μM 18β-GA; GA5) and 10 μM GA (200 μM H_2O_2 + 10 μM 18β-GA; GA10) groups. In brief, Schwann cells ($1.2x10^5$ cells/well) were cultivated in 6-well plates. The medium

Table I. Primer sequences used for PCR.

Gene	Forward primer (5'-3')	Reverse primer (5'-3')
TRPA1	AAATGCCACAGTTCTCAA	TCTTCGTGTTGCCCTTAT
TRPV1	TTCAAGGGTTCCACGAGA	AGTGCCGACACCTATCCA
TNF-α	GCGTGTTCATCCGTTCTCTACC	TACTTCAGCGTCTCGTGTGTTTCT
IL-1β	AGGAGAGACAAGCAACGACA	CTTTTCCATCTTCTTCTTTGGGTAT
β-actin	GAGAGGGAAATCGTGCGT	GGAGGAAGAGGATGCGG

TRPA1, transient receptor potential ankyrin 1; TRPV1, transient receptor potential vanilloid 1.

was then discarded and the cells were washed with PBS. The cells were then incubated with 18β-GA at 5 or 10 μM concentrations or SB203580 for 24 h. After the medium was discarded, the cells were washed with PBS and they were incubated with 200 μM H_2O_2 (dissolved in PBS) for 4 h at 37˚C.

Intracellular ROS measurement. An intracellular ROS measurement assay was performed as previously described (17). After being cultivated for 24 h, Schwann cells were incubated at 37˚C for 20 min in PBS containing 20 μM 2',7'-dichlorodihydrofluorescein diacetate (DCFH-DA). Subsequently, the cells were treated with 18β-GA at two fixed concentrations or SB203580 and then incubated with 200 μM H_2O_2 in PBS. After the PBS had been removed, intracellular ROS production was measured on an inverted fluorescence microscope. Photomicrographs of three fields were taken for each well. The amount of intracellular ROS was determined based on the fluorescence intensity via Image-Pro Plus 6.0 (Media Cybernetics, Inc.).

Hoechst 33258 staining. After pre-treatment and incubation with 200 μM H_2O_2 in PBS at 37˚C for 4 h, cells were incubated with Hoechst 33258 (5 μl in 1.0 ml of PBS) in each well for 20 min. After washing twice with PBS, fluorescence images were acquired using an inverted fluorescence microscope. Three photomicrographs were captured per well, and Image-Pro Plus 6.0 was used for analysis.

Cell apoptosis detection via flow cytometry. Annexin V FITC and propidium iodide (PI) were used to evaluate the apoptotic rates of Schwann cells in different groups. After pre-treatment, cells were incubated with 200 μM H_2O_2 in PBS at 37˚C for 4 h. Cells were collected with trypsin and washed with PBS. Subsequently, 1x10^6 cells were placed in binding buffer and double-stained with Annexin V FITC and PI in the dark for 15 min at 4˚C. The proportion of early + late apoptotic cells was then analysed on a flow cytometer (CytExpert 2.3; Beckman Coulter, Inc.) to determine the apoptotic rate.

Reverse-transcription quantitative (RT-qPCR). According to the manufacturer's protocol, total RNA was isolated using RNAiso Plus. Subsequently, cDNA was synthesized based on the instructions of the RT-PCR kit. Then, a Bio-Rad CFX96 Real-Time PCR System (Bio-Rad Laboratories, Inc.) was used to perform qPCR. The amplification parameters were 95˚C for 30 sec, followed by 40 cycles of 95˚C for 5 sec and 60˚C for 34 sec, 95˚C for 15 sec, 60˚C for 60 sec and 95˚C for 15 sec. The relative expression of mRNA was calculated by the $2^{-\Delta\Delta Cq}$ method (18) after normalization to β-actin. For this procedure, SYBR®-Green Premix qPCR and primers (Table I) were used.

Western blot analysis. Changes in the expression of Bcl-xl, Bcl-2, Bad, Bax, cleaved-caspase 3 and cleaved-caspase 7, which are related to apoptosis pathways, were assessed by western blot analysis. The levels of TRPA1 and TRPV1, which are closely related to injury, were also measured. RIPA buffer was used to lyse the cells and obtain the proteins from the supernatant. The protein concentration was determined via a BCA assay, and samples (30 μg) were separated via 4-10% SDS-PAGE followed by transfer to PVDF membranes and blocking with 5% skim milk at 37˚C for 1 h. PVDF membranes were incubated with primary antibody (1:1,000 dilution) overnight at 4˚C for 24 h and then with secondary antibody (1:5,000 dilution) for 45 min at 37˚C. Finally, chemiluminescence was used to visualize the bands for assessment of the images via Image-Lab 3.0 (Bio-Rad Laboratories, Inc.).

Statistical analyses. Values are expressed as the mean ± standard deviation. Experiments were repeated three times. GraphPad Prism 8 (GraphPad Software, Inc.) and SPSS 13.0 (SPSS, Inc.) software were used to perform statistical analysis. The data were analyzed by one-way ANOVA. Bonferroni's test was the post hoc test after ANOVA. $P<0.05$ was considered to indicate a statistically significant difference.

Results

Target of 18β-GA activity. Through PubChem, the SMILES annotation for 18β-GA was obtained, which is 'CC1(C2CCC3(C(C2(CCC1O)C)C(=O)C=C4C3(CCC5(C4CC(CC5)(C)C(=O)O)C)C)C)C'. This sequence was inputted into Swiss Target Prediction, the SEA Search Server and TargetNet, which identified 126 active targets. In addition, 15,327 targets associated with injury were identified. A total of 111 potential targets associated with 18β-GA for injury management were further identified. Targets of 18β-GA with potential for injury treatment were inputted into the STRING database along with the species. The top 10 pathways were ranked and are presented in Fig. 1. In a previous experiment, it was indicated that model rats with chronic constriction injury of the sciatic nerve exhibited increased inflammation (19).

Therefore, 'Inflammatory mediator regulation of TRP channels', was chosen for experimental verification.

Effects of H_2O_2 and 18β-GA on Schwann cell viability. H_2O_2 decreased cell viability in a concentration-dependent manner. A moderate response (~50%) was induced by 200 μM H_2O_2 (Fig. 2A). To examine the cytotoxicity of 18β-GA, Schwann cells were incubated with various doses of 18β-GA at 37˚C for 24 h. Cytotoxicity was determined based on the results of the CCK-8 assays. Treatment with 10 μM 18β-GA significantly increased cell viability (P<0.05; Fig. 2B), confirming that a suitable concentration had been used. The concentrations of 10 and 5 μM were subsequently applied to achieve a dose-effect relationship and it was more suitable to choose 5 μM than 7.5 μM 18β-GA.

18β-GA inhibits H_2O_2-induced ROS production in Schwann cells. To determine whether the cytoprotective effects of 18β-GA are an intracellular effect, it was investigated whether 18β-GA is able to be transported into Schwann cells to inhibit H_2O_2-induced intracellular radical production. In brief, cells were first stressed with 18β-GA; 20 μM DCFH-DA was then added before intracellular ROS levels were evaluated. In this way, as 18β-GA and H_2O_2 did not come into contact in the extracellular space, any reduction in ROS levels was attributed to an intracellular effect. Treatment of Schwann cells with H_2O_2 increased intracellular ROS levels compared with those of untreated cells. However, 18β-GA and SB203580 attenuated ROS accumulation. The difference in ROS production under treatment with 200 μM H_2O_2 with and without 18β-GA was significant (Fig. 3). These results indicated that 18β-GA and SB203850 are able to decrease H_2O_2-induced ROS production in Schwann cells.

Hoechst 33258 staining. To determine whether 18β-GA protects the nucleus from damage, nuclei were subjected to Hoechst 33258 staining. After H_2O_2 treatment, Schwann cells exhibited apoptotic nuclei, but pre-treatment with 18β-GA and SB203580 markedly abrogated these effects. 18β-GA and SB203580 inhibited the formation of apoptotic nuclei induced by H_2O_2 treatment (Fig. 4).

Flow cytometry results. Flow cytometry was performed to investigate whether 18β-GA protects Schwann cells against H_2O_2-induced apoptosis (Fig. 5). The proportion of apoptotic cells was obviously lower in the control group (4.34±0.27%) than in the model group (12.63±1.21%). In addition, the percentage of apoptotic cells was markedly lower in the group pre-treated with SB203580 or 5 or 10 μM 18β-GA (7.02±0.30, 4.83±0.55 and 4.88±0.50%, respectively) than in the model group (P<0.05). 18β-GA enabled the recovery of cell viability to its normal level. These results suggested that 18β-GA and SB203580 markedly inhibited H_2O_2-induced apoptosis.

mRNA levels of TRPA1, TRPV1, IL1β and TNF-α. To explore the mRNA expression of TRPV1, TRPA1, IL-1β and TNF-α, RT-qPCR analysis was applied (Fig. 6). The mRNA expression of TRPV1, TRPA1, IL-1β and TNF-α in the control group was evidently enhanced after treatment with H_2O_2 (P<0.05). By contrast, 18β-GA decreased the expression of these genes

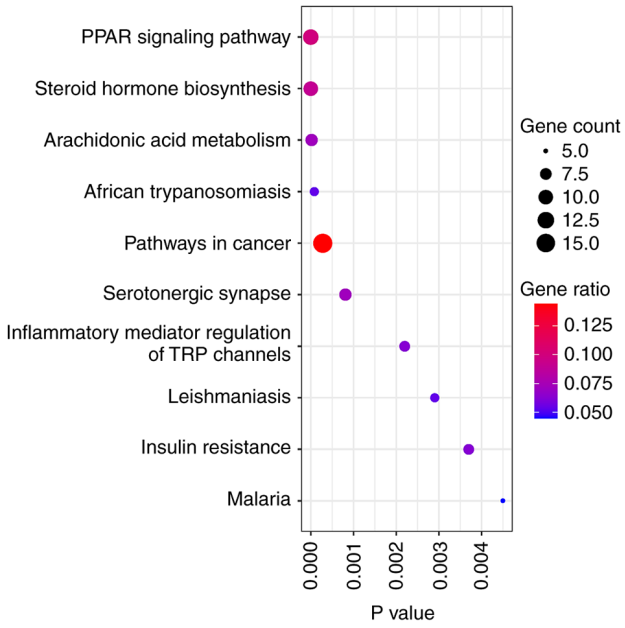

Figure 1. KEGG pathway analysis of target genes of 18β-GA. KEGG pathway enrichment analysis of 18β-GA targets with potential for treating damage was performed via DAVID. The top 10 pathways were ranked. KEGG, Kyoto Encyclopedia of Genes and Genomes; 18β-GA, 18β-glycyrrhetinic acid.

(P<0.05). The mRNA levels of the four genes returned to normal in the groups treated with SB203580 or 5 or 10 μM 18β-GA. Thus, 18β-GA had an anti-inflammatory effect.

Expression of TRP, apoptotic, antiapoptotic and p38 MAPK proteins. Western blot analysis was used to determine the expression of various proteins (Fig. 7). H_2O_2 decreased the expression of Bcl-2 and Bcl-xl (P<0.05), which are antiapoptotic proteins, while pre-treatment with 18β-GA abrogated the effect (P<0.05). Furthermore, H_2O_2 was indicated to increase the expression of Bax, Bad, cleaved-caspase-3 and cleaved-caspase-7 (P<0.05), which are proapoptotic proteins. Of note, in comparison to the H_2O_2-treated model group, SB203580 and 18β-GA enhanced the levels of Bcl-2 and Bcl-xl, and decreased the Bax, Bad, cleaved-caspase-3 and cleaved-caspase-7 levels (P<0.05), which were nearly normal.

The levels of TRPV1, TRPA1 and p-p38 MAPK in the model group were clearly increased after treatment with H_2O_2 (P<0.05). However, the p38 MAPK levels did not vary among the groups. 18β-GA and SB203580 reduced the expression of the three proteins compared with those in the model group (P<0.05). Furthermore, 18β-GA decreased TRPA1 to near-normal levels. However, SB203580 only slightly decreased the levels of TRPA1 and they remained significantly higher than those in the control group (P<0.05). Overall, the inhibitory effects of 18β-GA and SB203580 at different concentrations were similar, suggesting that 18β-GA was able to suppress the activation of p38 MAPK and the protein levels of TRPA1 and TRPV1.

Discussion

For network pharmacology research, the top 10 KEGG pathways are typically selected. In the present study, the pathway

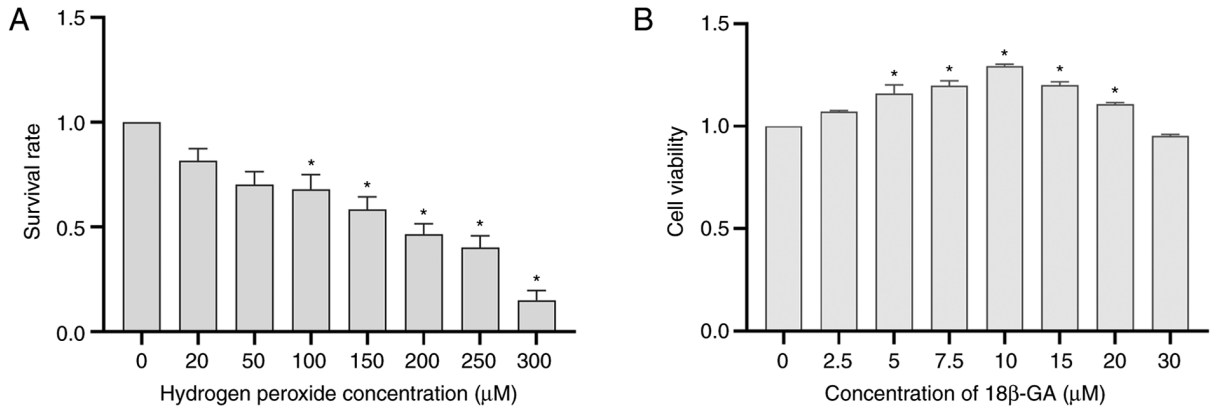

Figure 2. Cell viability and cytotoxicity assay. (A) H_2O_2 decreased cell viability in a concentration-dependent manner. (B) 18β-GA affected Schwann cell viability. *P<0.05 vs. control (0 μM H_2O_2 or 18β-GA). 18β-GA, 18β-glycyrrhetinic acid.

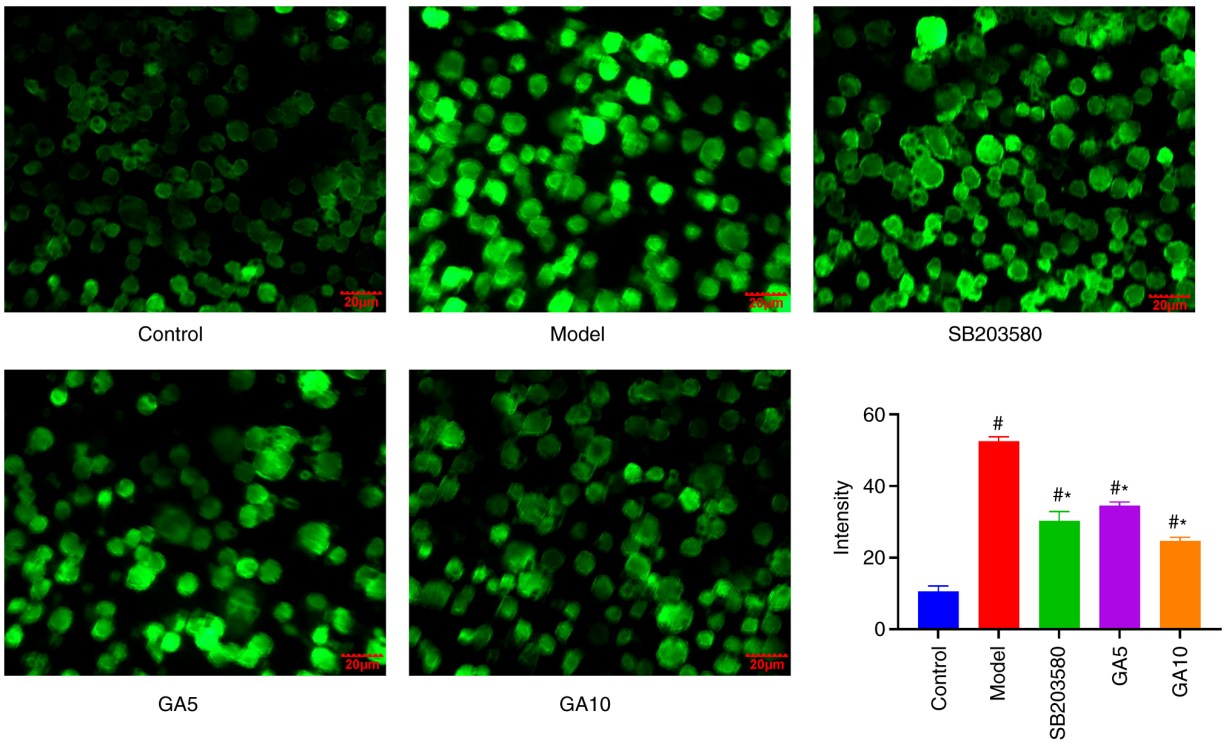

Figure 3. 18β-GA inhibits H_2O_2-induced ROS production. H_2O_2, 18β-GA and SB203580 affected the levels of intracellular ROS (scale bar, 20 μm). #P<0.05 vs. control group; *P<0.05 vs. model group. 18β-GA, 18β-glycyrrhetinic acid; ROS, reactive oxygen species; GA5, 5 μM 18β-GA; GA10, 10 μM 18β-GA. ROS, reactive oxygen species.

'Inflammatory mediator regulation of TRP channels' was selected, which contains IL-1β, phospholipase Cγ1 (PLCG1), protein kinase Cα (PRKCA), PRKCH, prostaglandin E receptor 2 (PTGER2), PTGER4 and TRPA1, for experimental verification. The experiments of the present study demonstrated that H_2O_2 induced oxidative stress and increased the proportion of apoptotic nuclei and the apoptotic rate in Schwann cells. H_2O_2 increased intracellular ROS and the levels of Bax, Bad, cleaved-caspase-3 and cleaved-caspase-7, while decreasing the levels of Bcl-2, Bcl-xl, TRPA1 and TRPV1 and p-p38 MAPK. In addition, H_2O_2 exposure increased the mRNA levels of TRPA1, TRPV1, IL-1β and TNF-α. However, pre-treatment with 18β-GA and SB203580 notably decreased the level of ROS and particularly prevented nuclear and Schwann cell apoptosis. In addition, pre-treatment with 18β-GA and SB203580 clearly reduced the protein levels of Bax, Bad, cleaved-caspase-3, cleaved-caspase-7, TRPA1, TRPV1 and p-p38 MAPK and the mRNA levels of TRPA1, TRPV1, IL-1β and TNF-α, and enhanced the levels of Bcl-xl and Bcl-2 in comparison with the model group.

Regarding the inflammatory pathway by which TRP channels are regulated, IL-1β, PLCG1, PRKCA, PRKCH, PTGER2 and PTGER4 are the upstream targets of TRPA1, as indicated in a signalling pathway on the official KEGG website (pathway map: map04750). Through this pathway of inflammation-mediated regulation of TRP channels, the expression of TRPA1 may be regulated by the p38 signalling pathway. Indeed, TRPA1 and TRPV1 are generally co-expressed in

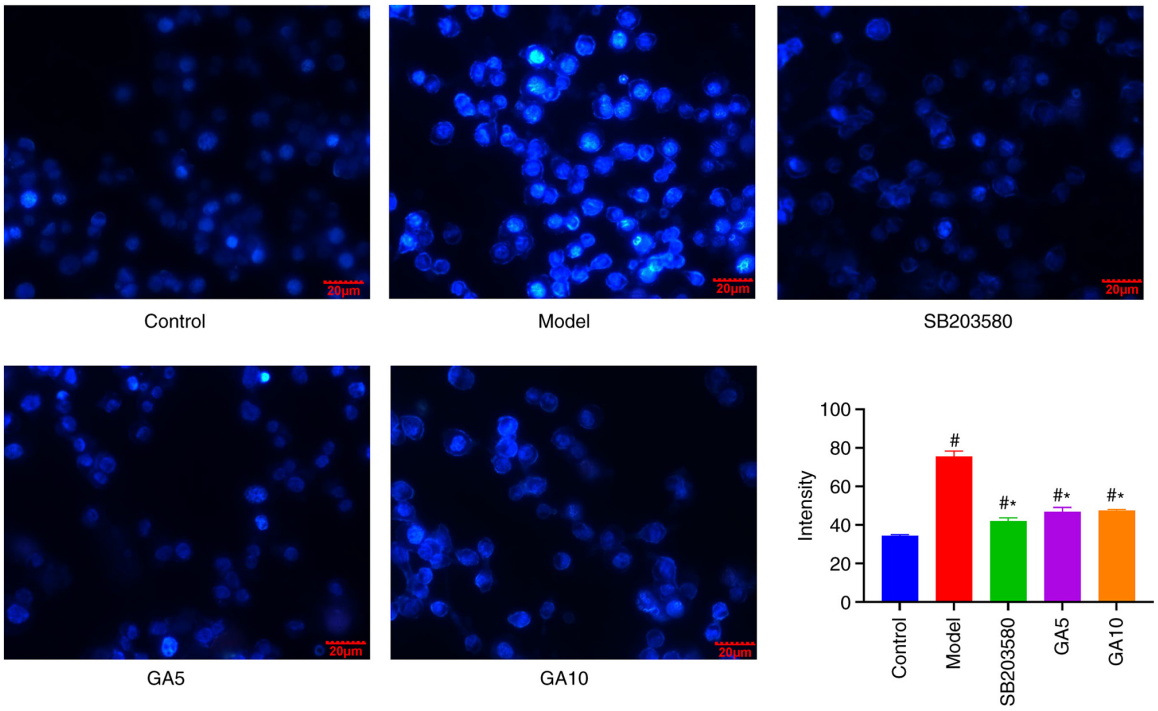

Figure 4. 18β-GA reverses H_2O_2-induced changes in condensed chromatin and apoptotic nuclei. H_2O_2, 18β-GA and SB203580 affected changes in the nuclei (scale bar, 20 μm). #P<0.05 vs. control group; *P<0.05 vs. model group. 18β-GA, 18β-glycyrrhetinic acid; GA5, 5 μM 18β-GA; GA10, 10 μM 18β-GA.

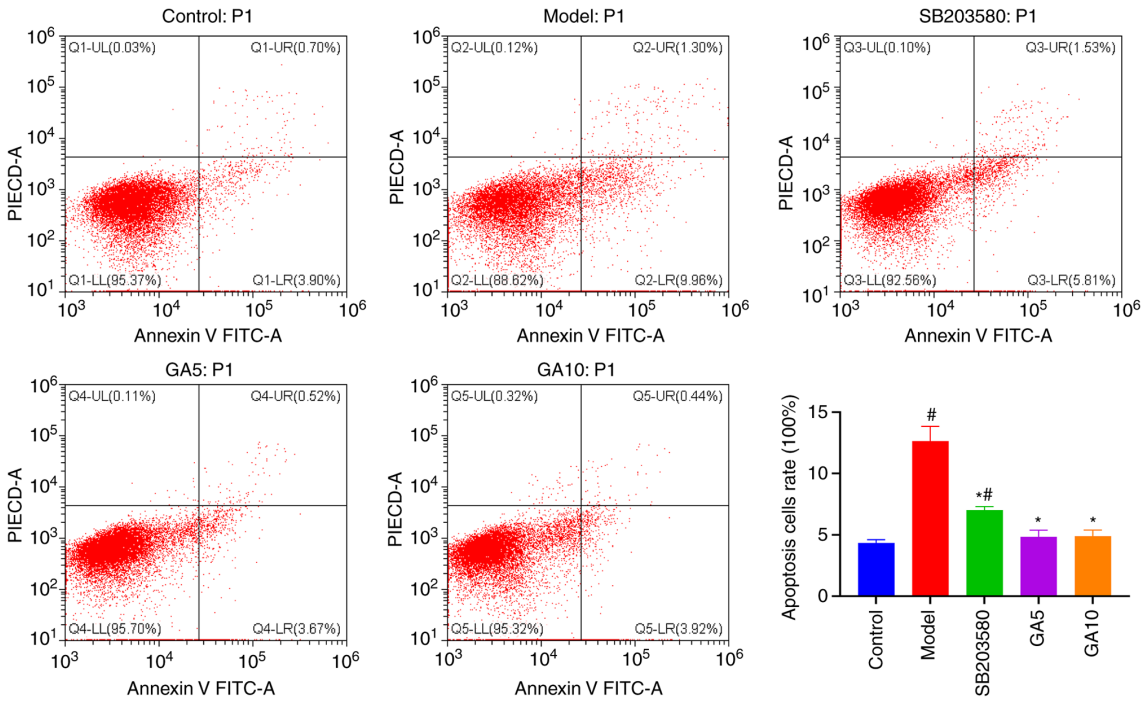

Figure 5. Protective effect of 18β-GA against H_2O_2-induced apoptosis. Flow cytometry revealed that H_2O_2, 18β-GA and SB203580 affected the levels of cell apoptosis. #P<0.05 vs. control group; *P<0.05 vs. model group. 18β-GA, 18β-glycyrrhetinic acid; PI, propidium iodide; Q, quadrant; UL, upper left; UR, upper right; LL, lower left; LR, lower right; GA5, 5 μM 18β-GA; GA10, 10 μM 18β-GA.

cells (20). Therefore, TRPA1, TRPV1 and p38 MAPK were selected as proteins from the inflammation-mediated regulation of the TRP channel pathway for analysis in the present study. According to differences in the expression levels determined by PCR and western blot analysis, a p38 inhibitor (SB203580) attenuated the H_2O_2-induced increase in TRPA1, TRPV1 and p-p38 MAPK at the protein level. These results suggested that TRPA1 and TRPV1 are related to injury and apoptosis. Furthermore, TRPA1 and TRPV1 were indicated to mediate cigarette smoke extract-induced damage by regulating oxidative stress, inflammatory infiltration and mitochondrial injury in bronchial epithelial cells (21).

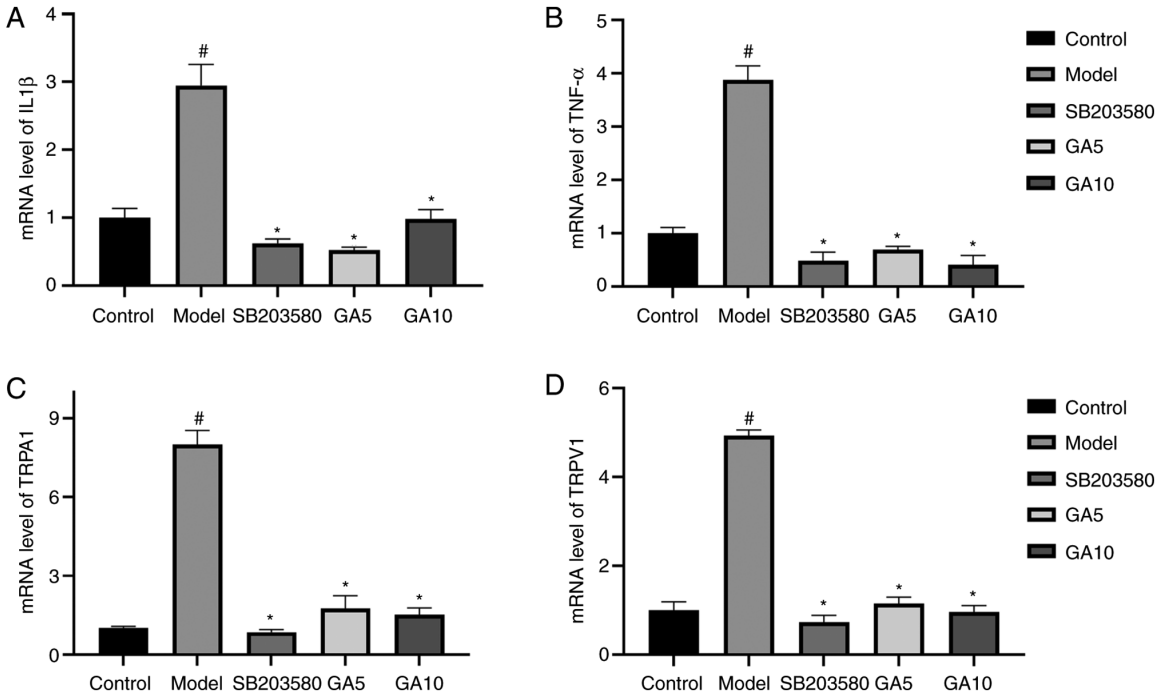

Figure 6. mRNA analysis of inflammatory markers. mRNA levels of (A) IL-1β, (B) TNF-α, (C) TRPA1 and (D) TRPV1 in the different groups determined by reverse transcription-quantitative PCR. #P<0.05 vs. control group; *P<0.05 vs. model group. 18β-GA, 18β-glycyrrhetinic acid; TRPA1, transient receptor potential ankyrin 1; TRPV1, transient receptor potential vanilloid 1; GA5, 5 μM 18β-GA; GA10, 10 μM 18β-GA.

Oxidative stress is involved in injury and apoptosis. The accumulation of ROS may result in various forms of oxidative protein, lipid and DNA modifications, leading to cellular damage. 18β-GA pre-treatment strongly regulated these oxidative conditions, and 18β-GA and SB203580 attenuated ROS accumulation. Previous studies demonstrated that Bcl-xl and Bcl-2 were associated with apoptosis induced by ROS accumulation (22); furthermore, ROS activate caspase-3 (22). Su *et al* (3) determined that 18β-GA treatment decreased the accumulation of ROS in RAW264.7 cells after exposure to X-ray radiation. SB203580 decreased the expression of cleaved-caspase 3 reduced the level of cleaved-caspase 7. SB203580 increased the expression of Bcl-xl and Bcl-2 after H_2O_2 treatment. In addition, the proportion of apoptotic cells was obviously lower in the group pre-treated with SB203580 than in the group pre-treated with H_2O_2 alone. Similarly, SB203580 reversed the increase in condensed chromatin and apoptotic nuclei after treatment with H_2O_2. Initial reports have suggested that p38 MAPK regulates mitochondria in drug-induced cancer cell apoptosis (23). These results are in agreement with the generally accepted knowledge that the inhibition of p38 MAPK phosphorylation prevents apoptosis (24). The p38 MAPK inhibitor SB202190 reduced TNF-α-induced TRPA1 expression.

Coskun *et al* (25) indicated that TNF-α induced tissue damage mediated by neutrophils. After treatment with H_2O_2, the mRNA levels of IL-1β and TNF-α increased sharply. Pre-treatment with 18β-GA reversed this trend. Previously, 18β-GA was reported to significantly inhibit lipopolysaccharide-induced TNF-α production (26). Ishida *et al* (27) indicated that the binding of hydroxypropyl-γ-cyclodextrin and 18β-GA had a negative effect on IL-6, IL-1β, TNF-α and mRNA expression and enhanced intestinal injury induced by indomethacin. Furthermore, Su *et al* (3) reported that 18β-GA inhibited radiation-induced inflammation by decreasing the accumulation of inflammatory cytokines, including IL-6 and IL-1β, caused by radiation. The results in the present study are similar to those of the aforementioned studies. Therefore, 18β-GA is able to attenuate the mRNA expression of TNF-α and IL1β, which may reduce the degree of cell apoptosis.

18β-GA increased the expression of Bcl-xl and Bcl-2 after H_2O_2 treatment and decreased the expression of Bax, Bad, cleaved-caspase-3 and cleaved-caspase-7. In addition, the proportion of apoptotic cells was notably higher in the group treated with H_2O_2 alone than in the group pre-treated with 18β-GA. 18β-GA similarly inhibited the protein levels of p-p38 MAPK. Su *et al* (3) indicated that 18β-GA exhibited anti-inflammatory activity against radiation-induced skin damage by inhibiting ROS accumulation and restricting the activation of the NF-κB and p38 MAPK pathways. The present results suggested that 18β-GA prevented Schwann cell injury and apoptosis induced by H_2O_2 via the p38 MAPK pathway.

There was no significant difference between 5 and 10 μM 18β-GA in terms of their anti-apoptosis effect and regulation of various signaling factors. These two concentrations were selected with the aim of obtaining a dose-effect relationship, but this was not achieved. A CCK-8 assay was used to detect cell viability. However, whilst this experiment indicates the toxicity of 18β-GA to cells, it may not reveal anti-damage effects of a compound; this may be the reason why the two concentrations of 18β-GA had the same effect.

The typical manifestations of peripheral nerve injury are increased oxidative stress (28,29), cell damage (28) and inflammatory infiltration (30). It was indicated that 18β-GA was able to alleviate these effects by decreasing inflammatory

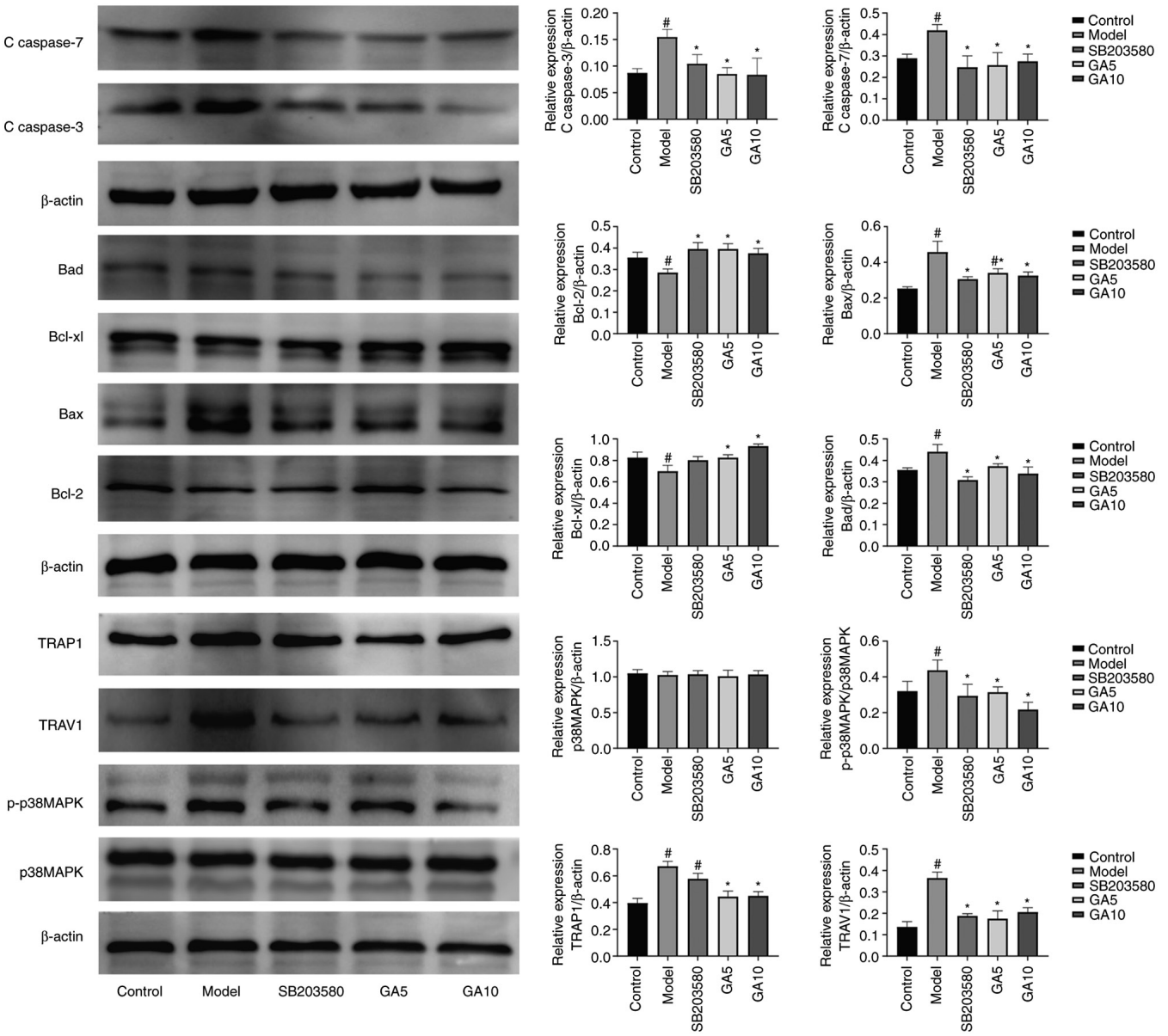

Figure 7. Expression of TRP, apoptotic, antiapoptotic and p38 MAPK proteins in different groups determined by western blot analysis. #P<0.05 vs. control group; *P<0.05 vs. model group. 18β-GA, 18β-glycyrrhetinic acid; TRPA1, transient receptor potential ankyrin 1; TRPV1, transient receptor potential vanilloid 1; p-p38, phosphorylated p38; GA5, 5 μM 18β-GA; GA10, 10 μM 18β-GA.

factors, decreasing the elevated expression of TRP proteins and inhibiting p38 MAPK phosphorylation.

However, there were limitations to the present *in vitro* experiments. Cell experiments are able to demonstrate that a drug has therapeutic potential for peripheral nerve injury prior to animal experiments. However, the main disadvantage of *in vitro* experimental research is that it is challenging to extrapolate the results to the biology of intact organisms, as the body is not a single-celled organism.

In conclusion, H_2O_2 increased intracellular ROS and the levels of Bax, Bad, cleaved-caspase-3 and cleaved-caspase-7 and decreased the levels of Bcl-xl and Bcl-2. Furthermore, H_2O_2 exposure increased the protein levels of TRPA1 and TRPV1 and the phosphorylation of p38 MAPK. 18β-GA and SB203580 attenuated ROS accumulation, inhibited the phosphorylation of p38 MAPK, enhanced the expression of Bcl-xl and Bcl-2 and decreased the levels of cleaved-caspase-7, cleaved-caspase-3, Bax and Bad, which indicated that 18β-GA may be a candidate drug to prevent peripheral nerve injury.

Acknowledgements

Not applicable.

Funding

This work was supported by the National Natural Science Foundation of China (grant no. 81874404).

Availability of data and materials

The datasets used and/or analyzed during the current study are available from the corresponding author on reasonable request.

Authors' contributions

DZ, JS, SC and GZ made considerable contributions to the experimental design, statistical data analysis and experimental procedures. XL, HS, BJ, YZ, YL, GQ and YP assisted with the English writing, and made substantial contributions towards the experimental design and statistical analysis. DZ and JS checked and confirmed the authenticity of the raw data. All authors read and approved the final manuscript.

Ethics approval and consent to participate

Not applicable.

Patient consent for publication

Not applicable.

Competing interests

The authors declare that they have no competing interests.

References

1. Pastorino G, Cornara L, Soares S, Rodrigues F and Oliveira MBPP: Liquorice (*Glycyrrhiza glabra*): A phytochemical and pharmacological review. Phytother Res 32: 2323-2339, 2018.
2. Abd El-Twab SM, Hozayen WG, Hussein OE and Mahmoud AM: 18β-glycyrrhetinic acid protects against methotrexate-induced kidney injury by up-regulating the Nrf2/ARE/HO-1 pathway and endogenous antioxidants. Ren Fail 38: 1516-1527, 2016.
3. Su L, Wang Z, Huang F, Lan R, Chen X, Han D, Zhang L, Zhang W and Hong J: 18β-glycyrrhetinic acid mitigates radiation-induced skin damage via NADPH oxidase/ROS/p38MAPK and NF-κB pathways. Environ Toxicol Pharmacol 60: 82-90, 2018.
4. Mahmoud AM, Hussein OE, Hozayen WG and Abd El-Twab SM: Methotrexate hepatotoxicity is associated with oxidative stress, and down-regulation of PPARγ and Nrf2: Protective effect of 18β-Glycyrrhetinic acid. Chem Biol Interact 270: 59-72, 2017.
5. Cheng X, Qiu L and Wang F: 18α-glycyrrhetinic acid (GA) ameliorates fructose-induced nephropathy in mice by suppressing oxidative stress, dyslipidemia and inflammation. Biomed Pharmacother 125: 109702, 2020.
6. Zhou J, Cai W, Jin M, Xu J, Wang Y, Xiao Y, Hao L, Wang B, Zhang Y, Han J and Huang R: 18β-glycyrrhetinic acid suppresses experimental autoimmune encephalomyelitis through inhibition of microglia activation and promotion of remyelination. Sci Rep 5: 13713, 2015.
7. Oztanir MN, Ciftci O, Cetin A, Durak MA, Basak N and Akyuva Y: The beneficial effects of 18β-glycyrrhetinic acid following oxidative and neuronal damage in brain tissue caused by global cerebral ischemia/reperfusion in a C57BL/J6 mouse model. Neurol Sci 35: 1221-1228, 2014.
8. Kao TC, Shyu MH and Yen GC: Glycyrrhizic acid and 18beta-glycyrrhetinic acid inhibit inflammation via PI3K/Akt/GSK3beta signaling and glucocorticoid receptor activation. J Agric Food Chem 58: 8623-8629, 2010.
9. Gao L, Feng A, Yue P, Liu Y, Zhou Q, Zang Q and Teng J: LncRNA BC083743 promotes the proliferation of Schwann cells and axon regeneration through miR-103-3p/BDNF after sciatic nerve crush. J Neuropathol Exp Neurol 79: 1100-1114, 2020.
10. Chi GF, Kim DW, Jiang MH, Yoon KJ and Son Y: Schwann-like cells from human melanocytes and their fate in sciatic nerve injury. Neuroreport 22: 603-608, 2011.
11. Wang L, Sanford MT, Xin Z, Lin G and Lue TF: Role of Schwann cells in the regeneration of penile and peripheral nerves. Asian J Androl 17: 776-782, 2015.
12. Gonçalves NP, Mohseni S, El Soury M, Ulrichsen M, Richner M, Xiao J, Wood RJ, Andersen OM, Coulson EJ, Raimondo S, *et al*: Peripheral nerve regeneration is independent from schwann cell $p75^{NTR}$ expression. Front Cell Neurosci 13: 235, 2019.
13. Gomez-Sanchez JA, Pilch KS, van der Lans M, Fazal SV, Benito C, Wagstaff LJ, Mirsky R and Jessen KR: After nerve injury, lineage tracing shows that myelin and remak schwann cells elongate extensively and branch to form repair Schwann cells, which shorten radically on remyelination. J Neurosci 37: 9086-9099, 2017.
14. Julien O and Wells JA: Caspases and their substrates. Cell Death Differ 24: 1380-1389, 2017.
15. Kalkavan H and Green DR: MOMP, cell suicide as a BCL-2 family business. Cell Death Differ 25: 46-55, 2018.
16. Li ZY, Tung YT, Chen SY and Yen GC: Novel findings of 18β-glycyrrhetinic acid on sRAGE secretion through inhibition of transient receptor potential canonical channels in high-glucose environment. Biofactors 45: 607-615, 2019.
17. Wankun X, Wenzhen Y, Min Z, Weiyan Z, Huan C, Wei D, Lvzhen H, Xu Y and Xiaoxin L: Protective effect of paeoniflorin against oxidative stress in human retinal pigment epithelium in vitro. Mol Vis 17: 3512-3522, 2011.
18. Livak KJ and Schmittgen TD: Analysis of relative gene expression data using real-time quantitative PCR and the 2(-Delta Delta C(T)) method. Methods 25: 402-408, 2001.
19. Zhang D, Sun J, Yang B, Ma S, Zhang C and Zhao G: Therapeutic effect of tetrapanax papyriferus and hederagenin on chronic neuropathic pain of chronic constriction injury of sciatic nerve rats based on KEGG pathway prediction and experimental verification. Evid Based Complement Alternat Med 2020: 2545806, 2020.
20. Gouin O, L'Herondelle K, Lebonvallet N, Le Gall-Ianotto C, Sakka M, Buhé V, Plée-Gautier E, Carré JL, Lefeuvre L, Misery L and Le Garrec R: TRPV1 and TRPA1 in cutaneous neurogenic and chronic inflammation: Pro-inflammatory response induced by their activation and their sensitization. Protein Cell 8: 644-661, 2017.
21. Wang M, Zhang Y, Xu M, Zhang H, Chen Y, Chung KF, Adcock IM and Li F: Roles of TRPA1 and TRPV1 in cigarette smoke-induced airway epithelial cell injury model. Free Radic Biol Med 134: 229-238, 2019.
22. Ma G, Luo W, Lu J, Ma DL, Leung CH, Wang Y and Chen X: Cucurbitacin E induces caspase-dependent apoptosis and protective autophagy mediated by ROS in lung cancer cells. Chem Biol Interact 253: 1-9, 2016.
23. Kang N, Wang MM, Wang YH, Zhang ZN, Cao HR, Lv YH, Yang Y, Fan PH, Qiu F and Gao XM: Tetrahydrocurcumin induces G2/M cell cycle arrest and apoptosis involving p38 MAPK activation in human breast cancer cells. Food Chem Toxicol 67: 193-200, 2014.
24. Sun Y, Liu WZ, Liu T, Feng X, Yang N and Zhou HF: Signaling pathway of MAPK/ERK in cell proliferation, differentiation, migration, senescence and apoptosis. J Recept Signal Transduct Res 35: 600-604, 2015.
25. Coskun AK, Yigiter M, Oral A, Odabasoglu F, Halici Z, Mentes O, Cadirci E, Atalay F and Suleyman H: The effects of montelukast on antioxidant enzymes and proinflammatory cytokines on the heart, liver, lungs, and kidneys in a rat model of cecal ligation and puncture-induced sepsis. ScientificWorldJournal 11: 1341-1356, 2011.
26. Ishida T, Mizushina Y, Yagi S, Irino Y, Nishiumi S, Miki I, Kondo Y, Mizuno S, Yoshida H, Azuma T and Yoshida M: Inhibitory effects of glycyrrhetinic acid on DNA polymerase and inflammatory activities. Evid Based Complement Alternat Med 2012: 650514, 2012.
27. Ishida T, Miki I, Tanahashi T, Yagi S, Kondo Y, Inoue J, Kawauchi S, Nishiumi S, Yoshida M, Maeda H, *et al*: Effect of 18β-glycyrrhetinic acid and hydroxypropyl γcyclodextrin complex on indomethacin-induced small intestinal injury in mice. Eur J Pharmacol 714: 125-131, 2013.
28. Khezri MK, Turkkan A, Koc C, Salman B, Levent P, Cakir A, Kafa IM, Cansev M and Bekar A: Anti-apoptotic and anti-oxidant effects of systemic uridine treatment in an experimental model of sciatic nerve injury. Turk Neurosurg 31: 373-378, 2021.
29. Zhang D, Yang B, Chang SQ, Ma SS, Sun JX, Yi L, Li X, Shi HM, Jing B, Zheng YC, *et al*: Protective effect of paeoniflorin on H_2O_2 induced Schwann cells injury based on network pharmacology and experimental validation. Chin J Nat Med 19: 90-99, 2021.
30. Kalinski AL, Yoon C, Huffman LD, Duncker PC, Kohen R, Passino R, Hafner H, Johnson C, Kawaguchi R, Carbajal KS, *et al*: Analysis of the immune response to sciatic nerve injury identifies efferocytosis as a key mechanism of nerve debridement. Elife 9: e60223, 2020.